J. Fluid Mech. (2001), *vol.* 432, *pp.* 387–408. Printed in the United Kingdom

Flow induced by a randomly vibrating boundary

By DMITRI VOLFSON[1] AND JORGE VIÑALS[1,2]

[1]Supercomputer Computations Research Institute, Florida State University, Tallahassee, FL 32306-4130, USA

[2] Department of Chemical Engineering, FAMU-FSU College of Engineering, Tallahassee, FL 31310-6046, USA

(Received 20 January 2000 and in revised form 7 August 2000)

We study the flow induced by random vibration of a solid boundary in an otherwise quiescent fluid. The analysis is motivated by experiments conducted under the low level and random effective acceleration field that is typical of a microgravity environment. When the boundary is planar and is being vibrated along its own plane, the variance of the velocity field decays as a power law of distance away from the boundary. If a low-frequency cut-off is introduced in the power spectrum of the boundary velocity, the variance decays exponentially for distances larger than a Stokes layer thickness based on the cut-off frequency. Vibration of a gently curved boundary results in steady streaming in the ensemble average of the tangential velocity. Its amplitude diverges logarithmically with distance away from the boundary, but asymptotes to a constant value instead if a low-frequency cut-off is considered. This steady component of the velocity is shown to depend logarithmically on the cut-off frequency. Finally, we consider the case of a periodically modulated solid boundary that is being randomly vibrated. We find steady streaming in the ensemble average of the first-order velocity, with flow extending up to a characteristic distance of the order of the boundary wavelength. The structure of the flow in the vicinity of the boundary depends strongly on the correlation time of the boundary velocity.

1. Introduction

This paper examines the formation of viscous layers in a fluid which is in contact with a solid boundary that is vibrated randomly. The analysis is motivated by the low level and random acceleration field that affects a number of microgravity experiments. We first study the case of a planar boundary to generalize the classical result of Stokes (1851) who considered a boundary vibrated periodically along its own plane. We next consider a slightly curved boundary, and show that steady streaming appears in the ensemble average at first order in the perturbed flow variables. There are several qualitative similarities and differences with the classical result by Schlichting (1932, 1979) for the case of periodic vibration. Finally, we address the case of a modulated boundary that is vibrated randomly.

Our study is primarily motivated by the significant levels of random residual accelerations (g-jitter) that have been detected during Space missions in which microgravity experiments have been conducted (Walter 1987; Nelson 1991; DeLombard *et al.* 1997). A better understanding of the response of a fluid to such disturbances would enable improved experiment design to minimize or compensate for their influence. We choose to focus here on the formation of viscous layers around solid boundaries when the flow amplitude has a random component. Potential microgravity applications include the dynamics of colloidal suspensions, coarsening studies of solid–liquid mixtures in which purely diffusive-controlled transport is desired, or the interaction between the viscous layer produced by bulk flow of random amplitude and the morphological instability of a crystal–melt interface. Our study represents the first step in this direction, and focuses on simple geometries in order to elucidate those salient features of the flow that arise from the random nature of the vibration.

Previous theoretical work on the influence of g-jitter on fluid flow ranges from order of magnitude estimates to detailed numerical calculations (Alexander 1990). The bulk of the research to date models the acceleration field by some simple analytic function in which the acceleration is typically decomposed into steady and time-dependent components, the latter being periodic in time (Gershuni & Zhukhovitskii 1976; Kamotani, Prasad & Ostrach 1981; Alexander, Ouazzani & Rosenberger 1991; Farooq & Homsy 1994; Grassia & Homsy 1998*a*, *b*; Gershuni & Lyubimov 1998). A few studies have also addressed the consequences of isolated pulses of short duration (Alexander *et al.* 1997). On the other hand, we follow the approach of Zhang, Casademunt & Viñals (1993) and Thomson *et al.* (1997) who adopted a statistical description of the residual acceleration field onboard spacecraft, and modelled the acceleration time series as a stochastic process in time. The main premise of this approach is that a statistical description is necessary in those cases in which the characteristic time scales of the physical process under investigation are long compared with the correlation time of g-jitter. The particular stochastic process used is narrow-band noise (Stratonovich 1967) which has been shown to describe reasonably well many of the features of g-jitter time series measured onboard Space Shuttle by Thomson *et al.* (1997). A theoretical advantage of narrow-band noise is that it provides a convenient way of interpolating between monochromatic noise (akin to studies involving a deterministic and periodic gravitational field), and white noise (in which no frequency component is preferred).

We discuss in this paper the flow induced in an otherwise quiescent fluid by the random vibration of a solid boundary. The velocity of the boundary $u_0(t)$ is assumed prescribed, and modelled as a narrow-band stochastic process. First, we consider an infinite planar boundary that is being vibrated along its own plane to generalize the classical problem studied by Stokes (1851). In the monochromatic limit, the variance of the velocity field decays exponentially away from the wall, with a characteristic decay length given by the Stokes layer thickness $\delta_s = (2\nu/\Omega)^{1/2}$, where ν is the kinematic viscosity of the fluid, and Ω is the angular frequency of vibration of the boundary. Since the equations governing the flow are linear, we are able to obtain an analytic solution describing transient layer formation in the stochastic case, but only in the neighbourhood of the white and monochromatic noise limits. We then show that for any finite correlation time the stationary variance of the tangential velocity asymptotically decays as the inverse squared distance from the wall, in contrast with the exponential decay in the deterministic case. This asymptotic behaviour originates from the low-frequency range of the power spectrum of the boundary velocity. The crossover from power-law to exponential decay is explicitly computed by introducing a low-frequency cut-off in the power spectrum.

We next investigate two additional geometries in which the equations governing fluid flow are not linear, and show that several of the generic features obtained for the case of a planar boundary still hold. In the first case, we generalize the analysis of Schlichting (1932, 1979) concerning secondary steady streaming. He found that the oscillatory motion of the boundary induces a steady secondary flow outside the viscous boundary layer even when the velocity of the boundary averages to zero. If the thickness of the Stokes layer, δ_s, and the amplitude of oscillation, a, are small compared with a characteristic length scale of the boundary L ($\delta_s \ll L$, $a \ll L$), then the generation of secondary steady streaming may be described as follows. Vibration of the rigid boundary gives rise to an oscillatory and non-uniform motion of the fluid. The flow is potential in the bulk, and rotational in the boundary layer because of no-slip conditions on the boundary. The bulk flow applies pressure at the outer edge of boundary layer, which does not vary across the layer. The non-uniformity of the flow leads to vorticity convection in the boundary layer through nonlinear terms. Both convection and the applied pressure drive vorticity diffusion, and thus induce secondary steady motion which does not vanish outside the boundary layer. In the simplest case in which the far-field velocity is a standing wave $U(x,t) = U(x)\cos(\Omega t)$, the tangential component of the secondary steady velocity is

$$u^{(s)} = -\frac{3}{4\Omega} U \frac{\mathrm{d}U}{\mathrm{d}x}, \tag{1.1}$$

where x is a curvilinear coordinate along the boundary. In fact, (1.1) serves as the boundary condition for the stationary part of the flow in the bulk. Similar conclusions were later reached by Batchelor (1967) who studied sinusoidal oscillations of non-uniform phase, and by Gershuni & Lyubimov (1998) who studied monochromatic oscillations of a general form.

The second geometry that we address is the so-called wavy wall (Lyne 1971). The deterministic limit in which a wavy boundary is being periodically vibrated has been studied by a number of authors, mainly to address the interaction between the flow above the sea bed and ripple patterns on it (Lyne 1971; Kaneko & Honjii 1979; Vittori 1989; Blondeaux & Vittori 1994 and references therein). Lyne (1971) deduced the existence of steady streaming in the limit in which the amplitude of the wall deviation from planarity is small compared with the thickness of the Stokes layer. He introduced a conformal transformation and obtained an explicit solution in the limit of small kRe, where k is the wavenumber of the wall profile scaled by the thickness of the Stokes layer, and Re is the Reynolds number. The detailed structure of the secondary flow depends on the ratio between the wavelength of the boundary profile and the thickness of the Stokes layer.

In §§ 3 and 4, we discuss how the results for these two geometries generalize to the case of stochastic vibration. Section 3 addresses the flow created by a gently curved solid boundary that is being vibrated randomly. The perturbation parameter that we use is the ratio between the amplitude of vibration and the characteristic inverse curvature of the wall. The ensemble average of the stream function is not zero, and hence there exists stationary streaming in the stochastic case as well. The average velocity diverges logarithmically away from the boundary because of the low-frequency range of the power spectrum. We again introduce a low-frequency cut-off ω_c in the spectrum, and study the dependence of the stationary streaming on the cut-off frequency. We compute the stationary tangential velocity as a function of $\omega_c \ll 1$ and arbitrary β, and find a weak (logarithmic) singularity as $\omega_c \to 0$.

Section 4 discusses the formation of a boundary layer around a wavy boundary that is vibrated randomly. Positive and negative vorticity production in adjacent regions of the boundary introduces a natural decay length in the solution, thus leading to exponential decay of the flow away from the boundary, even in the absence of a low-frequency cut-off in the power spectrum of the boundary velocity. Steady streaming is found at second order comprising two or four recirculating cells per period of the boundary profile. The number of cells depends on the scaled correlation time $\Omega\tau$.

2. Randomly vibrating planar boundary

We first examine the case of a planar boundary that is being vibrated along a fixed direction on its own plane. In this case the governing equations are considerably simpler than in the more general geometries discussed in §§ 3 and 4. In particular, the Navier–Stokes equation is linear, a fact that allows a complete solution of the flow. Nevertheless, this simple solution still exhibits several of the qualitative features that are present in the case of random forcing by a curved boundary, namely asymptotic power law decay of the velocity field away from the boundary, and sensitive dependence on the low-frequency range of the power spectrum of the boundary velocity.

Consider an infinite solid boundary located at $z = 0$, and an incompressible and viscous fluid that occupies the region $z > 0$. The Navier–Stokes equation, and boundary conditions are

$$\partial_t u = \nu \partial_z^2 u, \tag{2.1}$$

$$u(0,t) = u_0(t), \quad u(\infty, t) < \infty, \tag{2.2}$$

where z is the coordinate normal to the boundary, $u(z,t)$ is the x component of the velocity, and $u_0(t)$ is the prescribed velocity of the boundary. The solution for harmonic vibration $u_0(t) = u_0 \cos(\Omega t)$ was given by Stokes (1851). It is a transversal wave that propagates into the bulk fluid with an exponentially decaying amplitude,

$$u(z,t) = u_0 e^{-z/\delta_s} \cos(\Omega t - z/\delta_s), \tag{2.3}$$

where $\delta_s = (2\nu/\Omega)^{1/2}$ is the Stokes layer thickness.

2.1. *Narrow-band noise*

As discussed in the introduction, the main topic of this paper is to examine how the nature of the bulk flow changes when the boundary velocity $u_0(t)$ is a random process. Specifically, we consider a Gaussian process defined by

$$\langle u_0(t) \rangle = 0, \quad \langle u_0(t) u_0(t') \rangle = \langle u_0^2 \rangle e^{-|t-t'|/\tau} \cos \Omega (t - t'). \tag{2.4}$$

This process is known as narrow-band noise (Stratonovich 1967). It is defined by three independent parameters: its variance $\langle u_0^2 \rangle$, its dominant angular frequency Ω, and the correlation time τ. Each realization of this random process can be viewed as a sequence periodic functions of frequency Ω, with amplitude and phase that remain constant for a time interval τ on average. White noise is recovered when $\Omega\tau \to 0$ while $D = \langle {u_0}^2 \rangle \tau$ remains finite, whereas the monochromatic noise limit corresponds to $\Omega\tau \to \infty$, with $\langle u_0^2 \rangle$ finite. Monochromatic noise is akin to a single-frequency periodic signal of the same frequency, but with randomly drawn amplitude and phase. The relationship between the two can be illustrated by considering a deterministic function $x(t) = x_0 \cos(\Omega t)$ and defining the temporal average as

$$\langle x(t) x(t') \rangle = \lim_{T \to \infty} \frac{1}{T} \int_0^T dt \, x(t) x(t') = \frac{x_0^2}{2} \cos(\Omega (t - t')). \tag{2.5}$$

This average coincides with the ensemble average of the noise when $\langle u_0^2 \rangle = x_0^2/2$. The power spectrum corresponding to the correlation function (2.4) is

$$P(\omega) = \frac{\langle u_0^2 \rangle}{2\pi} \left[\frac{\tau}{1 + \tau^2(\omega - \Omega)^2} + \frac{\tau}{1 + \tau^2(\omega + \Omega)^2} \right]. \tag{2.6}$$

We will also use the spectral density of the process $u_0(t)$,

$$\hat{u}_0(\omega) = \frac{1}{2\pi}\int_{-\infty}^{\infty} \mathrm{d}t\, u_0(t)\mathrm{e}^{-\mathrm{i}\omega t}, \tag{2.7}$$

so that its ensemble average and correlation function are respectively given by

$$\langle \hat{u}_0(\omega)\rangle = 0, \quad \langle \hat{u}_0(\omega)\hat{u}_0^*(\omega')\rangle = \delta(\omega-\omega')P(\omega), \tag{2.8a,b}$$

and $*$ denotes complex conjugation. We will often use dimensionless variables in which $\langle u_0^2\rangle/\Omega$ is the scale of $P(\omega)$, and Ω is the angular frequency scale. In dimensionless form,

$$P(\omega,\beta) = \frac{1}{2\pi}\left[\frac{\beta}{1+\beta^2(\omega-1)^2} + \frac{\beta}{1+\beta^2(\omega+1)^2}\right], \tag{2.9}$$

where $\beta = \Omega\tau$. We have $\int_{-\infty}^{\infty} \mathrm{d}\omega P(\omega,\beta) = 1$, independent of β, and also $\lim_{\beta\to\infty} P(\omega) = [\delta(\omega-1)+\delta(\omega+1)]/2$. Note that the power spectrum does not vanish at small frequencies. Instead, $P(0,\beta) = \beta/\pi(1+\beta^2)$, which for large and small β behaves as $P(0,\beta) \sim 1/\pi\beta$ and $P(0,\beta) \sim \beta/\pi$ respectively. We will discuss separately the effect of this low-frequency contribution on the results presented in the remainder of the paper.

2.2. *Stationary variance for narrow-band noise*

While it is possible to obtain a closed analytic solution for the transient evolution of the variance $\langle u(z,t)^2\rangle$ when the vibration of the boundary is either monochromatic or white noise (see Appendix A), this is not the case when $u_0(t)$ is given by a general narrow-band process. It is possible, however, to obtain the stationary variance of the velocity. First, choose $1/\Omega$ as the time scale, $(\nu/\Omega)^{1/2}$ as the length scale, and $(\langle u_0^2\rangle)^{1/2}$ as the velocity scale. Then, (2.1) can be rewritten in Fourier space as

$$\mathrm{i}\omega\hat{u}(z,\omega) = \partial_z^2\hat{u}(z,\omega) \tag{2.10}$$

with

$$u(z,t) = \int_{-\infty}^{\infty} \mathrm{d}\omega\, \hat{u}(z,\omega)\mathrm{e}^{\mathrm{i}\omega t}. \tag{2.11}$$

The boundary conditions are, $\hat{u}(0,\omega) = \hat{u}_0(\omega)$, and $\hat{u}(z,\omega) < \infty$ at $z\to\infty$. The solution of (2.10) with these boundary conditions is

$$\hat{u}(z,\omega) = \mathrm{e}^{-\alpha z}\hat{u}_0(\omega), \qquad \alpha(\omega) = (1+\mathrm{i}\,\mathrm{sign}(\omega))(|\omega|/2)^{1/2}. \tag{2.12}$$

After some straightforward algebra we find

$$\frac{\langle u^2(z,\beta)\rangle}{2} = I(z,\beta) = \int_0^{\infty} \mathrm{d}\omega P(\omega,\beta)\exp(-z(2\omega)^{1/2}). \tag{2.13}$$

We have also used the fact that the power spectrum (2.9) is even in frequency.

We next analyse the asymptotic dependence of $I(z,\beta)$ at large z. In this limit, $I(z,\beta)$ mainly depends on the low-frequency region of the power spectrum; higher frequencies are suppressed by the exponential factor. By using Watson's lemma (Nayfeh 1981), we find

$$I(z,\beta) = \frac{\beta}{\pi(1+\beta^2)}\frac{1}{z^2} + \frac{30\beta^3(3\beta^2-1)}{\pi(1+\beta^2)^3}\frac{1}{z^6} + O(z^{-10}). \tag{2.14}$$

This asymptotic form at large z is valid for all β. In particular, the dominant behaviour for small and large β is $I(z,\beta) \sim \beta/\pi z^2$ and $I(z,\beta) \sim 1/\pi\beta z^2$ respectively.

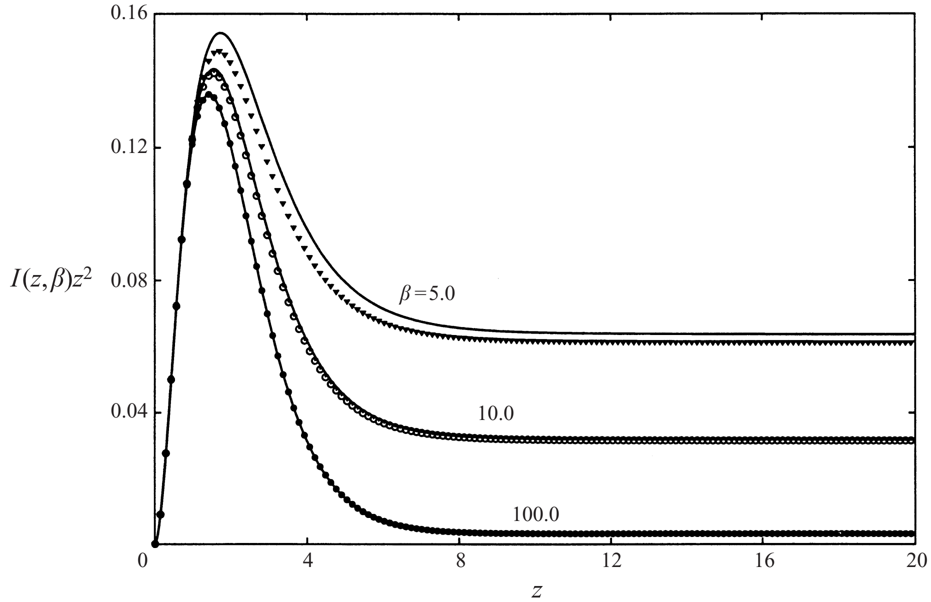

FIGURE 1. Normalized variance of the tangential velocity for the case of a planar boundary computed by numerical integration of (2.13) (symbols), and its uniform asymptotic expansion, (2.15), (solid lines). The function $I(z,\beta)\,z^2$ asymptotes to a constant value outside the classical Stokes layer based on Ω. The uniform expansion remains a good approximation even for moderate β.

We can also find the asymptotic behaviour at large β that is uniformly valid in z,

$$I(z,\beta) = \frac{e^{-\xi}}{2} - \frac{\xi}{2\pi\beta}\left(\mathrm{Ci}(\xi)\sin(\xi) - \mathrm{Si}(\xi)\cos(\xi) - \tfrac{1}{2}(e^{-\xi}\mathrm{Ei}(\xi) - e^{\xi}\mathrm{Ei}(-\xi))\right) + O(\beta^{-3}), \tag{2.15}$$

where $\xi = \sqrt{2}z$, Ci and Si denote the integral sine and cosine functions, and Ei stands for the exponential integral function (Gradshteyn & Ryzhik 1980). For $z \lesssim 1$, the variance decreases exponentially. At larger z, the exponential terms in (2.15) become small, so that the remaining asymptotic dependence for large z is given by (2.14). The quantity $I(z,\beta)\,z^2$ computed both from (2.13) and the uniform expansion (2.15) is presented in figure 1. For fixed β, $I(z,\beta)$ asymptotes to $\beta/\pi(1+\beta^2)$ outside the Stokes layer. This value is the coefficient of the leading term in the asymptotic expansion (2.14). The expansion (2.15) is a good approximation even for moderate values of β.

To summarize, the variance of the velocity field does not decay exponentially away from the wall for finite β, but rather as the inverse squared distance. The crossover length separating exponential and power law decay increases with increasing β.

2.3. *Low-frequency cut-off in the power spectrum*

The coefficient of the leading term in (2.14) is in fact the value of $P(0,\beta) = \beta/\pi(1+\beta^2)$. The algebraic decay of $\langle u^2(z,\beta)\rangle$ follows from the diffusive nature of (2.1), and a non vanishing value of $P(\omega,\beta)$ as $\beta \to 0$. Before we analyse in §§3 and 4 how this behaviour is modified by nonlinearities in the governing equations, we explicitly address here the consequences of a low-frequency cut-off in the power spectrum. Of course, there always exists in practice a low-frequency cut-off because of limited observation time. Furthermore, the low-frequency range of the power spectrum of the residual acceleration field in microgravity ($\Omega/2\pi < 10^{-3}$Hz) is fairly difficult to measure reliably. We therefore introduce an effective cut-off frequency in the power spectrum, $\omega_c \ll 1$, and study the dependence of $\langle u^2(z,\beta)\rangle$ on ω_c. The stationary value of variance of the velocity is now given by

$$\frac{\langle u^2(z,\beta,\omega_c)\rangle}{2} = I_c(z,\beta,\omega_c) = \int_{\omega_c}^{\infty} \mathrm{d}\omega P(\omega,\beta)\exp\left(-z(2\omega)^{1/2}\right). \tag{2.16}$$

By using Watson's lemma, we find for large z

$$I_c(z,\beta,\omega_c) = \frac{\beta \exp\left(-z(2\omega_c)^{1/2}\right)}{\pi(1+\beta^2)}\left(\frac{1}{z^2} + \frac{(2\omega_c)^{1/2}}{z} + \text{h.o.t.}\right), \tag{2.17}$$

where h.o.t. stands for terms which are of higher order than terms retained under the assumption that both $1/z$ and $(2\omega_c)^{1/2}$ are small but independent. For $z \gg 1$, but $z(2\omega_c)^{1/2} \ll 1$ the dominant term in (2.17) is

$$I_c(z,\beta,\omega_c) \sim \frac{\beta}{\pi(1+\beta^2)}\frac{1}{z^2}, \quad z(2\omega_c)^{1/2} \ll 1. \tag{2.18}$$

On the other hand, if $z(2\omega_c)^{1/2} \geqslant 1$, the leading-order term is now a function of $\zeta = z(2\omega_c)^{1/2}$

$$I_c(z,\beta,\omega_c) \sim \frac{2\beta\omega_c\,\mathrm{e}^{-\zeta}}{\pi(1+\beta^2)}\left(\frac{1}{\zeta} + \frac{1}{\zeta^2}\right), \quad \zeta \geqslant 1. \tag{2.19}$$

Equations (2.18) and (2.19) show that at distances that are large compared with the thickness of the Stokes layer based on the dominant frequency Ω, $\langle u^2(z,\beta)\rangle$ decays algebraically with z. There exists, however, a length scale $z \sim O((2\omega_c)^{-1/2})$ beyond which the decay is exponential. This new characteristic length scale is the thickness of the Stokes layer based on the cut-off frequency. This conclusion appears natural given the principle of superposition for the linear differential equation (2.1).

We next address a specific functional form of the power spectrum at low frequencies that allows us to estimate analytically the resulting asymptotic dependence of the velocity variance.† Consider a power spectrum that at low frequencies is proportional to a power of the frequency

$$P(\omega) \sim A|\omega|^{\gamma}, \quad |\omega| \ll 1, \tag{2.20}$$

where A is a constant (narrow-band noise is the special case of $\gamma = 0$). Given this asymptotic form of the power spectrum, Watson's lemma gives the following asymptotics for the variance:

$$I(z) \sim \frac{\Gamma(2\gamma+2)}{2^{\gamma}}\frac{A}{z^{2\gamma+2}}, \quad z \gg 1,$$

where $\Gamma(x)$ is the standard Gamma function. The variance of the velocity field still decays as a power law of the distance away from the boundary as long as $\gamma > -1$, with an exponent that depends explicitly on γ. For $\gamma = -1$, the power spectrum diverges as ω^{-1} at small frequencies and the variance of the velocity field saturates to a constant.

From our analysis of the planar boundary in this Section, we conclude that the asymptotic behaviour of the velocity variance can be exponential or a power law depending on the low-frequency range of the power spectrum. As we show later in this paper, the asymptotic decay obtained in this case is crucial in determining the

† We are indebted to an anonymous reviewer for this suggestion.

structure of the secondary stationary flows that appear when nonlinear terms are incorporated into the analysis.

3. Streaming due to random vibration

Next we investigate to what extent the results of § 2 hold in configurations in which the governing equations are not linear. We examine in this section the flow induced by a gently curved solid boundary that is being randomly vibrated. The boundary velocity is assumed to be described by a narrow-band stochastic process, and hence our results will reduce to Schlichting's in the limit of infinite correlation time. However, for finite values of β the results are qualitatively different. Vorticity produced at the vibrating boundary penetrates into the bulk fluid already at zeroth order. Depending on the low-frequency range of the power spectrum of the boundary velocity, this may result in a logarithmic divergence of the ensemble average of the first-order velocity with distance away from the wall.

Define the following dimensionless quantities:

$$\left.\begin{aligned} z = \tilde{z}[(\nu/\Omega)^{1/2}], \quad x = \tilde{x}[L], \quad t = \tilde{t}[\Omega^{-1}], \quad \psi = \tilde{\psi}[(2\langle u_0^2\rangle \nu/\Omega)^{1/2}], \\ \epsilon = (2\langle u_0^2\rangle)^{1/2}/\Omega L, \quad Re^2 = 2\langle u_0^2\rangle/\Omega\nu, \quad \tilde{\Delta} = \partial_{\tilde{z}}^2 + \epsilon^2/Re^2\partial_{\tilde{x}}^2 \end{aligned}\right\} \tag{3.1}$$

Assume now that the characteristic linear scale of the boundary L is large so that ϵ is a small quantity. If the Reynolds number Re remains finite, then we have $\nu/\Omega L^2 \ll 1$. We next write the governing equations and boundary conditions in the frame of reference co-moving with the solid boundary and obtain for a two-dimensional geometry (tildes are omitted)

$$\partial_t\Delta\psi + \epsilon\frac{\partial(\psi,\Delta\psi)}{\partial(z,x)} = \Delta^2\psi, \tag{3.2}$$

$$\psi = 0, \quad \partial_z\psi = 0 \quad \text{at} \quad y = 0, \tag{3.3a,b}$$

$$\partial_z\psi = 2^{-1/2}U(x)u_0(t) \quad \text{at} \quad z = \infty, \tag{3.4}$$

where x, z are the tangential and normal coordinates along the boundary, and ψ is the stream function, $\boldsymbol{u} = (\partial_z\psi, -\partial_x\psi)$. We have also used the notation $\partial(a,b)/\partial(z,x) = (\partial_z a)(\partial_x b) - (\partial_x a)(\partial_z b)$ for the nonlinear term. The far-field boundary condition is a non-uniform and random velocity field, of the order of $\langle u_0^2\rangle^{1/2}$, with a spatially non-uniform amplitude $U(x)$, and a stochastic modulation $u_0(t)$ which is a Gaussian stochastic process with zero mean, and narrow-band power spectrum. We first expand the stream function as a power series of ϵ, $\psi = \psi_0 + \epsilon\psi_1 + \dots$ and solve (3.2) order by order.

At order ϵ^0 we obtain the following equation:

$$(\partial_t\partial_z^2 - \partial_z^4)\psi_0 = 0 \tag{3.5}$$

with boundary conditions

$$\psi_0 = 0, \quad \partial_z\psi = 0 \quad \text{at} \quad z = 0, \tag{3.6a,b}$$

$$\partial_z\psi = 2^{-1/2}U(x)u_0(t) \quad \text{at} \quad z = \infty. \tag{3.7}$$

At this order, the equations effectively describe the flow induced above a planar boundary with a far-field velocity boundary condition that is not uniform. The solution can be found by Fourier transformation. We define

$$\psi_0(x,z,t) = \int_{-\infty}^{\infty} \mathrm{d}\omega\, \hat{\psi}_0(x,z,\omega)\mathrm{e}^{\mathrm{i}\omega t}. \tag{3.8}$$

The transformed (3.5) and the transformed boundary conditions (3.6*a,b*) allow separation of variables. We define

$$\hat{\psi}_0(x,z,\omega) = 2^{-1/2}U(x)\hat{u}_0(\omega)\hat{\zeta}_0(z,\omega),$$

so that (3.5) leads to

$$(\mathrm{i}\omega\partial_z^2 - \partial_z^4)\hat{\zeta}_0 = 0, \tag{3.9}$$

with boundary conditions $\hat{\zeta}_0 = 0$, $\partial_z\hat{\zeta}_0 = 0$, at $z = 0$ and $\partial_z\hat{\zeta}_0 = 1$ at $z = \infty$. The solution is

$$\hat{\zeta}_0(z,\omega) = -1/\alpha + z + 1/\alpha \mathrm{e}^{-\alpha z}, \quad \alpha(\omega) = (1 + \mathrm{i}\,\mathrm{sign}(\omega))(|\omega|/2)^{1/2}). \tag{3.10}$$

At order ϵ we find

$$(\partial_t\partial_z^2 - \partial_z^4)\psi_1 = \partial_x\psi_0\partial_z^3\psi_0 - \partial_z\psi_0\partial_x\partial_z^2\psi_0 \tag{3.11}$$

with boundary conditions $\psi_1 = 0$, $\partial_z\psi_1 = 0$ at $z = 0$. The remaining boundary condition for ψ_1 needs to be discussed separately. Consider first the classical deterministic limit which can be formally obtained by setting $\beta = \infty$. Then, the right-hand side of (3.11) involves stationary terms (of zero frequency), and sinusoidal terms with twice the frequency of the far-field flow. Since the equation is linear, the solution ψ_1 has exactly the same temporal behaviour. In this case, it is known that it is not possible to find a solution for $\partial_z\psi_1$ that vanishes at large z, but only one that simply remains bounded as $z \to \infty$. By analogy, we introduce a similar requirement in the stochastic case of $\beta < \infty$. Since the zeroth-order stream function diverges linearly, this condition simply amounts to requiring that the expansion in powers of ϵ remains consistent.

We now take the ensemble average of (3.11), and consider the long-time stationary limit of the average ($\psi_1^{(s)} = \lim_{t\to\infty}\langle\psi_1\rangle$), to find

$$\partial_z^4\psi_1^{(s)} = \left\langle \partial_z\psi_0\partial_x\partial_z^2\psi_0 - \partial_x\psi_0\partial_z^3\psi_0 \right\rangle. \tag{3.12}$$

This equation can be integrated from infinity to z. We obtain

$$\partial_z^3\psi_1^{(s)} = \frac{U}{2}\frac{\mathrm{d}U}{\mathrm{d}x}F(z,\beta), \tag{3.13}$$

where

$$F(z,\beta) = \int_0^{\infty} \mathrm{d}\omega P(\omega,\beta)Q(\omega,z),$$

and

$$Q(\omega,z) = (-2 + 2\partial_z\hat{\zeta}_0\partial_z\hat{\zeta}_0^* - \hat{\zeta}_0\partial_z^2\hat{\zeta}_0^* - \hat{\zeta}_0^*\partial_z^2\hat{\zeta}_0).$$

The power spectrum $P(\omega,\beta)$ is defined in (2.9). The constant that appears in the expression for $Q(\omega,z)$ comes from the pressure gradient imposed at infinity.

We now proceed to solve (3.13) subject to the boundary conditions $\psi_1^{(s)} = \partial_z\psi_1^{(s)} = 0$ on the solid boundary, and $\partial_z^2\psi_1^{(s)} \to 0$ as $z \to \infty$. This is a boundary value problem for $\psi_1^{(s)}$ which, in the limit $\beta \to \infty$, can be solved analytically. The result obtained by Schlichting is recovered, namely that the solution may be bounded at infinity simply by setting the divergent component of the homogeneous part of the solution equal to zero to satisfy the principle of minimal singularity (Van Dyke 1964). Otherwise $\partial_z \psi_1^{(s)}$ is singular *a fortiori*. Since we cannot find an complete analytic solution for finite β, we proceed as follows. We recast the boundary value problem as an initial value problem, and search for a boundary condition on $\partial_z^2 \psi_1^{(s)}$ at $z = 0$ so that the homogeneous part of the solution remains bounded. This boundary condition can be found analytically by integrating (3.13) from 0 to z. We find

$$\partial_z^2 \psi_1^{(s)}(z) - \partial_z^2 \psi_1^{(s)}(0) = \frac{U}{2}\frac{\mathrm{d}U}{\mathrm{d}x} \int_0^z \mathrm{d}z' \int_0^\infty \mathrm{d}\omega P(\omega, \beta) Q(\omega, z'),$$

or after changing the order of integration,

$$\partial_z^2 \psi_1^{(s)}(z) - \partial_z^2 \psi_1^{(s)}(0) = \frac{U}{2}\frac{\mathrm{d}U}{\mathrm{d}x} \int_0^\infty \mathrm{d}\omega P(\omega, \beta) \left[\int^z \mathrm{d}z' Q(\omega, z') - \left(\int^z \mathrm{d}z' Q(\omega, z') \right)_{z=0} \right].$$

The second integral within brackets equals $(2/\omega)^{1/2}$. In order to avoid a linear divergence of $\partial_z \psi_1^{(s)}(z)$ we equate the constant terms on both sides, thus obtaining the third initial condition

$$\begin{aligned} \partial_z^2 \psi_1^{(s)}(0, \beta) &= U \frac{\mathrm{d}U}{\mathrm{d}x} \frac{2^{1/2}}{2} \int_0^\infty \mathrm{d}\omega\, \omega^{-1/2} P(\omega, \beta) \\ &= U \frac{\mathrm{d}U}{\mathrm{d}x} \frac{(2\beta)^{1/2}}{4q} ((2(q-\beta))^{1/2} + (q+1)^{1/2} + (q-1)^{1/2}), \end{aligned} \qquad (3.14)$$

where $q = (1+\beta^2)^{1/2}$, and the dependence of initial condition on β is shown explicitly. Equation (3.13) with its original boundary conditions, supplemented with (3.14) is an initial value problem, which we have solved numerically.

Before presenting the numerical results, we study the asymptotic behaviour of the solution for large z which is determined by the asymptotic form of $F(z, \beta)$ at large z. By explicit substitution of the zeroth-order solution we find

$$Q(z, \omega) = (-4 \cos(Z) - 2Z(\cos(Z) + \sin(Z)) + 2 \sin(Z)) \mathrm{e}^{-Z} + 2\mathrm{e}^{-2Z}, \qquad (3.15)$$

where $Z = z(\omega/2)^{1/2}$. The leading contribution to $F(z, \beta)$ as $z \to \infty$ originates from the zero-frequency limit of $P(\omega, \beta)$. Thus $F(z, \beta) \sim P(0, \beta) \int_0^\infty \mathrm{d}\omega Q(\omega, z)$. The remaining integral may be easily calculated to yield the asymptotic form

$$F(z, \beta) \sim \frac{6\beta}{\pi(1+\beta^2)} \frac{1}{z^2}. \qquad (3.16)$$

Therefore the stationary mean first-order velocity $u_1^{(s)} = \partial_z \psi_1^{(s)}$ has a logarithmic asymptotic form (see (3.13)).

We have numerically calculated $\partial_z \psi_1^{(s)}(z)$ for a range of values of β. The results are presented in figure 2. Equation (3.13) was integrated numerically with no-slip boundary conditions for $\psi_1^{(s)}$, and (3.14). The numerical results support our conclusion about the logarithmic divergence of $u_1^{(s)}$ with distance for any finite β. As β increases the stationary mean velocity profile approaches a limiting form that corresponds to the monochromatic limit of $\beta \to \infty$. In this limit we recover the Schlichting result, according to which $\partial_z \psi_1^{(s)}(z)$ asymptotes to a constant value over a distance of the order of the deterministic Stokes layer.

It is however important to discuss at this point the range of validity of our solution. At $O(\epsilon), \tilde{\Delta} \simeq \partial_{\tilde{z}}^2$, independent of the second derivative along the tangential coordinate, and hence of the curvature of the boundary. At this order we find that $u_1^{(s)}$ is proportional to $\ln z$. At distances $z \sim L$, second derivatives along the tangential

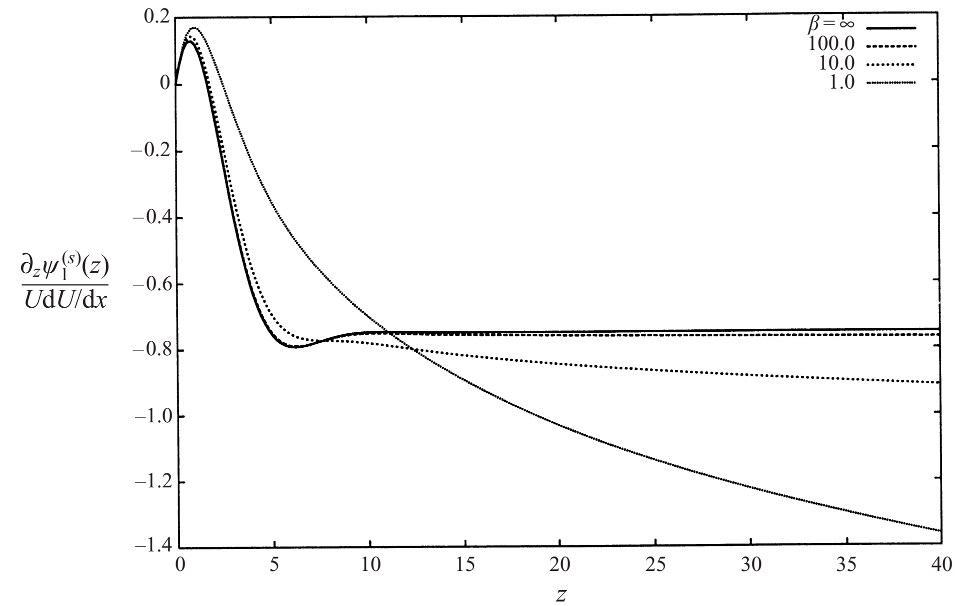

FIGURE 2. Stationary first-order velocity as a function of distance for a range of values of β. All curves diverge logarithmically at large z, except for $\beta = \infty$ (monochromatic limit), in which case the velocity asymptotes to a constant within the Stokes layer. This latter behaviour reproduces the classical result of Schlichting.

direction will no longer be negligible compared to normal derivatives, and our $O(\epsilon)$ calculation breaks down. We expect that at the next order in ϵ the logarithmic divergence beyond distances $z \sim L$ will be suppressed. This is analogous to our numerical result in § 4 concerning the vibration of a wavy wall when the wavelength of the boundary is much larger than the Stokes layer thickness. There we find an intermediate region in which the tangential velocity grows logarithmically with z, crossing over to exponential decay for distances larger than the wavelength.

Finally, we expect that our results hold when the weakly curved solid boundary considered in our analysis has a non-zero normal component of the velocity. This component would only enter the determination of the outer flow, which we do not need to compute. Hence the perturbation expansion remains essentially unchanged.

3.1. *Low-frequency cut-off in the power spectrum*

In § 2, we showed that a low-frequency cut-off in $P(\omega, \beta)$ led to an exponential decay of the velocity outside an effective boundary layer of thickness determined by the cut-off frequency. We therefore examine here the consequences of a low-frequency cut-off on the divergent behaviour of the stationary average of the first-order stream function. In order to find the asymptotic form of $\partial_z \psi_1^{(s)}$, we first integrate (3.13) twice. By using the low-frequency cut-off defined in § 2.3, we write

$$\partial_z \psi_1^{(s)}(z, \beta, \omega_c) = \frac{U}{2} \frac{\mathrm{d}U}{\mathrm{d}x} \left[G_c(z, \beta, \omega_c) - G_c(0, \beta, \omega_c) \right], \tag{3.17}$$

with,

$$G_c(z, \beta, \omega_c) = \int^z \mathrm{d}z' \int_\infty^{z'} \mathrm{d}z'' F_c(z'', \beta, \omega_c),$$

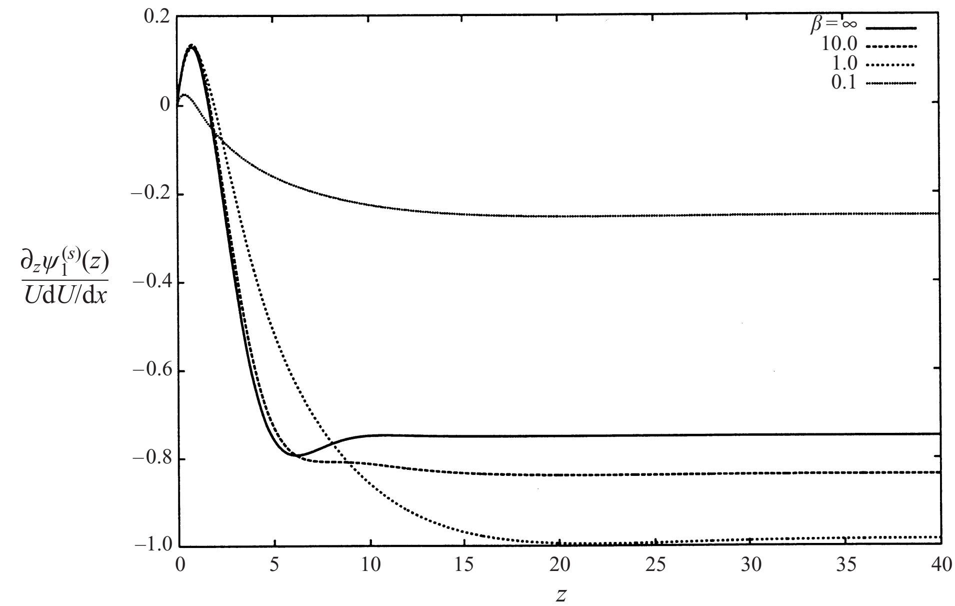

FIGURE 3. Stationary first-order velocity as a function of distance for a range of values of β. The power spectrum of the boundary velocity has a low-frequency cut-off at $\omega_c = 0.05$. The velocity asymptotes to a constant that depends on the value of β.

and,

$$F_c(z, \beta, \omega_c) = \int_{\omega_c}^{\infty} \mathrm{d}\omega P(\omega, \beta) Q(\omega, z).$$

If we set $\omega_c = 0$ and consider the monochromatic limit of $\beta \to \infty$, we find that $G_c(z, \infty, 0)$ contains an exponential factor that vanishes at $z \sim O(1)$, and that $G_c(0, \infty, 0) = 3/2$. Therefore the Schlichting result is recovered. An explicit form of $G_c(z, \beta, \omega_c)$ for any β and ω_c can be obtained analytically, but it is far too complicated and we do not quote it here. Figure 3 shows our result for $u_1^{(s)}(z)$ for fixed ω_c and a range of values of β. Its functional dependence is similar to that given for the planar boundary, and contains exponential terms involving $(-z\omega_c^{1/2})$. It is also of interest to find the asymptotic value of the velocity away from the boundary. We find that $\partial_z \psi_1^{(s)}(\infty, \beta, \omega_c) = -(U\mathrm{d}U/2\mathrm{d}x)\, G_c(0, \beta, \omega_c)$. For finite but small ω_c, we obtain

$$\partial_z \psi_1^{(s)}(\infty, \beta, \omega_c) = -\frac{3}{4} U \frac{\mathrm{d}U}{\mathrm{d}x} \frac{\beta}{\pi(1+\beta^2)} \left(2\beta \arctan(\beta) - \ln \left(\frac{\beta^2 \omega_c^2}{1+\beta^2} \right) \right) + O(\omega_c^2). \quad (3.18)$$

The analytic and numerical values of the tangential mean stationary velocity at large distances as a function of the cut-off frequency are given in figure 4. Computations were done as described in the previous section, and for different values of $\omega_c \ll 1$ and β. In all cases $\partial_z \psi_1^{(s)}$ reached constant values at large enough z (the numerical value of infinity, z_∞, was chosen so that the change in velocity for $z \geqslant z_\infty$ was less than a prescribed tolerance). We also checked that any change in the boundary condition (3.14) leads to a linear divergence in the tangential mean stationary velocity, thus confirming the adequacy of this boundary condition. The figure also shows that the computed values of $\partial_z \psi_1^{(s)}(z = \infty, \beta, \omega_c)$ for small ω_c are in a good agreement with (3.18).

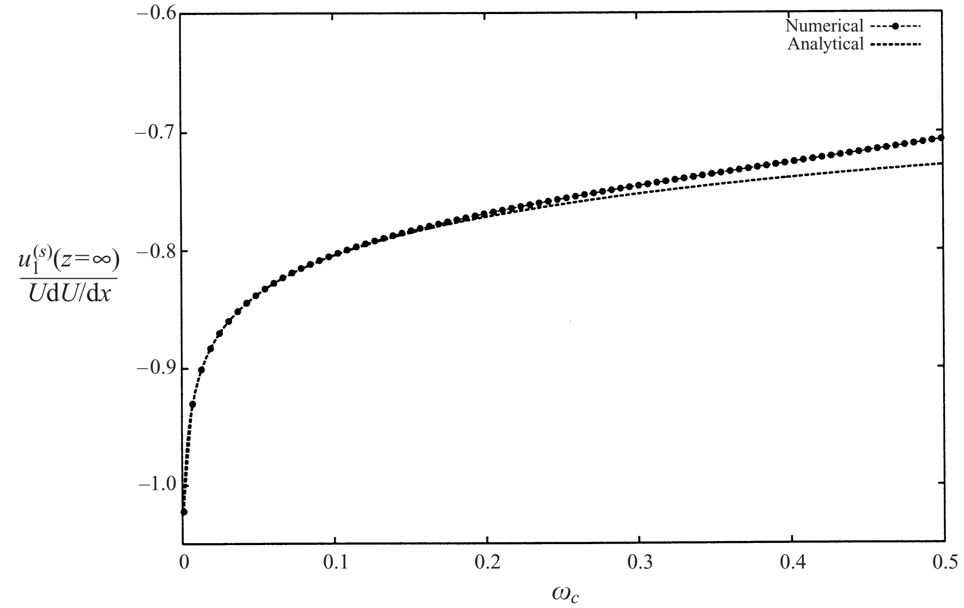

FIGURE 4. Asymptotic dependence of the stationary velocity on the cut-off frequency ω_c. We show the case $\beta = 10$ given by (3.18) along with the numerically obtained solution.

In summary, (3.18) shows that the tangential velocity away from the boundary asymptotes to a constant that is a function of β, and has a weak (logarithmic) dependence on the cut-off frequency ω_c. Therefore the asymptotic dependence in the stochastic case (with a cut-off) and in the deterministic case are qualitatively similar, although the value of the asymptotic velocity of the former depends on β. Note also that this asymptotic behaviour only sets in for distances larger than $(\nu/\omega_c\Omega)^{1/2}$, a value that can be quite large in practical microgravity conditions.

Finally we explore the large-z asymptotics for a power spectrum of the form (2.20). According to the results of § 2.3, the asymptotic dependence of the variance of the velocity field in the planar boundary case is identical to that of the body force $F(z,\beta)$ in (3.13). Therefore, at large distances

$$\partial_z^3 \psi_1^{(s)} \sim \frac{U}{2}\frac{\mathrm{d}U}{\mathrm{d}x}\frac{\tilde{A}}{z^{2\gamma+2}},$$

where $\tilde{A}$ is a constant. At fixed x, the resulting tangential velocity for $\gamma > 0$ is

$$\partial_z \psi_1^{(s)} \sim \frac{U}{2}\frac{\mathrm{d}U}{\mathrm{d}x}\left(-a + \frac{b}{z^{2\gamma}}\right),$$

where $a = 3\int_0^\infty \mathrm{d}\omega\, \omega^{-1} P(\omega) > 0$ and $b = \tilde{A}/2\gamma(2\gamma+1)$ are constants, and logarithmic for $\gamma = 0$. This power-law decay is also to be interpreted as intermediate asymptotics, valid for distances smaller than the characteristic linear scale of the boundary.

4. Randomly vibrating wavy boundary

In the two previous sections we considered cases in which the characteristic linear scale of the solid boundary was either infinite or large compared with the Stokes layer thickness, based on the dominant frequency. We examine here the case of a wavy boundary and study how comparable length scales in both directions influence the flow away from the boundary. In contrast with the Schlichting problem, the external applied flow is now uniform or, alternatively, the length scale over which the flow is not uniform is much larger than the wavelength of the boundary. Thus one anticipates that the normal component of the flow that appears is caused by the wall profile. This flow interacts through nonlinear terms with the externally forced flow that is parallel to the average profile of the boundary and gives rise to stationary streaming. Even for stochastic vibration we show that positive and negative vorticity production in adjacent regions of the boundary introduces a natural decay length in the zeroth-order solution, thus leading to exponential decay of the flow away from the boundary, even in the absence of a low-frequency cut-off in the power spectrum of the boundary velocity.

Consider a rigid wavy wall being washed by a uniform oscillatory flow parallel to the wall wave vector,

$$\boldsymbol{u}(x, z=\infty) = (u_0(t), 0). \tag{4.1}$$

We now assume that $u_0(t)$ is a narrow-band Gaussian process. Assume also that the amplitude of the boundary modulation l is small compared with both the Stokes layer δ_s and the wavelength L, with δ_s/L finite. The following dimensionless quantities are introduced:

$$\left.\begin{array}{l} z = \tilde{z}[(\nu/\Omega)^{1/2}], \quad x = \tilde{x}[(\nu/\Omega)^{1/2}], \quad t = \tilde{t}[\Omega^{-1}], \quad \psi = \tilde{\psi}[(2\left\langle u_0^2\right\rangle \nu/\Omega)^{1/2}], \\ \epsilon = l/(\nu/\Omega)^{1/2}, \quad Re = \left[2\left\langle u_0^2\right\rangle/\Omega\nu\right]^{1/2}, \quad k = 2\pi(\nu/\Omega)^{1/2}/L, \quad \tilde{\Delta} = \partial_{\tilde{z}}^2 + \partial_{\tilde{x}}^2 \end{array}\right\} \tag{4.2}$$

referred to the Cartesian coordinate system sketched in figure 5. The solid boundary is located at

$$\epsilon\eta(x) = \epsilon(\hat{\eta}\,\mathrm{e}^{\mathrm{i}kx} + \mathrm{c.c.}) \tag{4.3}$$

with constant complex amplitude $\hat{\eta}$ so that $|\hat{\eta}| = 1/2$. The dimensionless (and two-dimensional) Navier–Stokes equation (tildes are omitted in what follows) reads

$$\partial_t \Delta\psi + Re\frac{\partial(\psi, \Delta\psi)}{\partial(z, x)} = \Delta^2\psi, \tag{4.4}$$

with no-slip conditions at the boundary,

$$\psi = 0, \quad \partial_z\psi = 0 \quad \text{at} \quad y = \epsilon\eta(x), \tag{4.5a,b}$$

and the imposed uniform flow at infinity,

$$\partial_x\psi = 0, \quad \partial_z\psi = 2^{-1/2}u_0(t) \quad \text{at} \quad z = \infty. \tag{4.6a,b}$$

These equations depend only on three dimensionless parameters: ϵ, the ratio of the amplitude of the wavy wall to the boundary layer width, Re the Reynolds number, representing the ratio of the amplitude of boundary oscillations to the Stokes layer thickness, and k the wavenumber of the wall profile in units of boundary layer width. We assume $\epsilon \ll 1$ and expand the stream function in a power series of ϵ,

$$\psi = \psi_0 + \epsilon\psi_1 + \dots\,. \tag{4.7}$$

The boundary conditions are likewise expanded in power series of ϵ,

$$\psi(z)|_{z=\eta} = \psi_0(z)|_{z=0} + \epsilon(\psi_1(z)|_{z=0} + \eta\partial_z\psi_0(z)|_{z=0}) + \dots\,. \tag{4.8}$$

We now solve (4.4) order by order in ϵ.

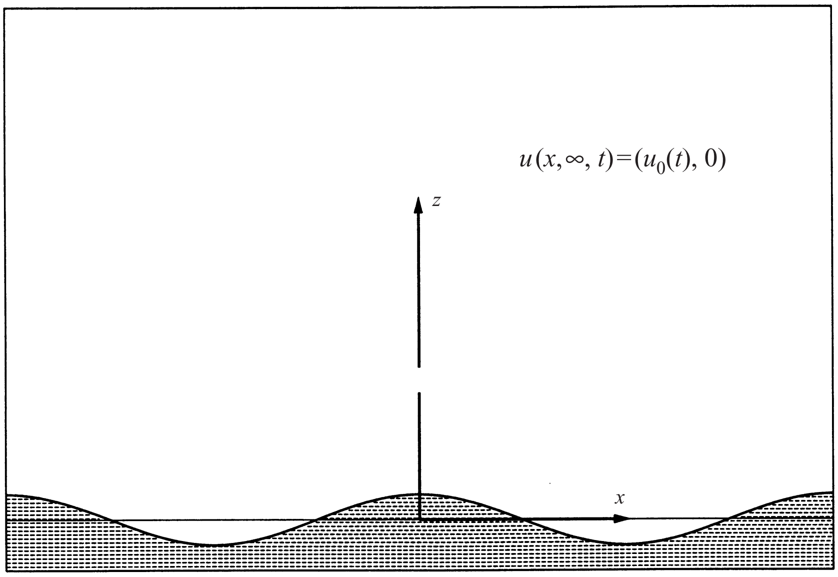

FIGURE 5. Schematic view of the geometry of the wavy wall studied in §4.

At zeroth order the wall is effectively planar. We decompose the Fourier transform of the stream function as, $\hat{\psi}_0(x,z,\omega) = 2^{-1/2}\hat{u}_0(\omega)\hat{\zeta}_0(z,\omega)$. The function $\hat{\zeta}_0(z,\omega)$ is given in (3.10). At this order, the solution is identical to that found for a planar boundary.

At first order we seek a solution of the form

$$\psi_1 = \hat{\eta}\,\exp(ikx)\phi(z,t) + \text{c.c.} \tag{4.9}$$

so that the amplitude $\phi(z,t)$ satisfies the Orr–Sommerfeld equation (see Blondeaux & Vittori 1994),

$$(\partial_t\mathscr{D} - \mathscr{D}^2)\phi = ikRe(\partial_z^3\psi_0 - \partial_z\psi_0\mathscr{D})\phi, \quad \mathscr{D} = \partial_z^2 - k^2, \tag{4.10}$$

with non-homogeneous boundary conditions,

$$\phi = 0, \quad \partial_z\phi = -\partial_z^2\psi_0 \quad \text{at} \quad z = 0, \tag{4.11a,b}$$

$$\phi = 0, \quad \partial_z\phi = 0 \quad \text{at} \quad z = \infty, \tag{4.12a,b}$$

The linear operator on the left-hand side of (4.10) contains a significant difference with respect to that of (3.11), the equation governing the first-order stream function for the case of a slightly curved boundary. Both equations describe vorticity diffusion, but the biharmonic equation (4.10) contains a cut-off through the parameter k. It is precisely this term that will lead to an asymptotic exponential decay of the velocity field sufficiently far away from the boundary for any finite β. The exponential decay at long distances arises from the screening introduced by the simultaneous positive and negative vorticity produced at the troughs and crests of the wavy wall.

In order to obtain a solution of the Orr–Sommerfeld equation (4.10), we further expand the amplitude $\phi(z,t)$ in power series of $kRe = 2\pi(2\langle u_0^2\rangle)^{1/2}/L\Omega$. This is the ratio between the amplitude of oscillation of the flow at infinity and the wall wavelength. We write

$$\phi = \phi_0 + \mathrm{i}kRe\phi_1 + \ldots \,. \tag{4.13}$$

The function ϕ_0 obeys the linearized (4.10) with boundary conditions as in (4.11*a,b*)–(4.12*a,b*) with ϕ replaced by ϕ_0. The Fourier transform of ϕ_0 is given by

$$\hat{\phi}_0(z,\omega) = (2)^{-1/2}\hat{u}_0(\omega)\frac{\alpha}{\rho - k}\left(\mathrm{e}^{-\rho z} - \mathrm{e}^{-kz}\right), \tag{4.14}$$

with $\rho \equiv (\alpha^2 + k^2)^{1/2}$, and the principal branch of the square root is assumed ($\mathrm{Re}\{\rho\} > 0$). Recall that $\alpha = (1 + \mathrm{i}\,\mathrm{sign}(\omega))(|\omega|/2)^{1/2}$. The field ϕ_0 describes vorticity diffusion near the wavy wall caused by the uniform but oscillatory far-field flow. Both the spatial and ensemble averages of this flow are zero. However, the flow non-uniformity at $O(1)$ induces mean flow at $O(kRe)$, as it is readily apparent from the equation for ϕ_1,

$$(\partial_t\mathscr{D} - \mathscr{D}^2)\phi_1 = (\partial_z^3\psi_0 - \partial_z\psi_0\mathscr{D})\phi_0, \tag{4.15}$$

with boundary conditions $\phi_1 = 0$, $\partial_z\phi_1 = 0$ at $z = 0, \infty$. The field ϕ_1 describes vorticity diffusion forced by the nonlinear interaction between ϕ_0 and ψ_0. As was the case in § 3, we focus on the long-time limit of the ensemble average of (4.15), $\phi_1^{(s)} = \lim_{t\to\infty}\langle\phi_1\rangle = \chi + \text{c.c.}$, where χ is given by

$$\mathscr{D}^2\chi = -\tfrac{1}{2}G(z,\beta), \tag{4.16}$$

with

$$\left.\begin{aligned} G(z,\beta) &= \int_0^\infty \mathrm{d}\omega\, P(\omega,\beta)\, Q(z,\omega,\beta),\\ Q(z,\omega,\beta) &= \alpha(\rho + k)(2\mathrm{e}^{-(\alpha^*+\rho)z} - \mathrm{e}^{-(\alpha^*+k)z} - \mathrm{e}^{-\rho z}). \end{aligned}\right\} \tag{4.17}$$

The corresponding boundary conditions are homogeneous, $\chi = 0$, $\partial_z\chi = 0$ at $z = 0, \infty$. The solution is

$$\left.\begin{aligned} \chi(z,\beta) &= \int_0^\infty \mathrm{d}\omega\, P(\omega,\beta)\hat{\chi}(z,\omega),\\ \hat{\chi}(z,\omega) &= A_1\mathrm{e}^{-\rho z} + A_2\mathrm{e}^{-(\alpha^*+\rho)z} + A_3\mathrm{e}^{-(\alpha^*+k)z} + (B_1 + zB_2)\mathrm{e}^{-kz}, \end{aligned}\right\} \tag{4.18}$$

where the functions A_i, B_i depend on frequency and wavenumber,

$$\left.\begin{aligned} &A_1 = D/\alpha^4, \quad A_2 = D/(2\alpha^2\rho^2), \quad A_3 = -D/(\alpha^2(\alpha^* + 2k)^2, \quad D = \alpha(\rho + k)/2,\\ &B_1 = -(A_1 + A_2 + A_3), \quad B_2 = (\rho - k)A_1 + (\rho + \alpha^* - k)A_2 + \alpha^* A_3. \end{aligned}\right\} \tag{4.19}$$

Therefore the stationary part of the averaged first-order stream function is given by

$$\psi_1^{(s)} = \mathrm{i}kRe\hat{\eta}\,\exp(\mathrm{i}kx)(\chi + \chi^*) + \text{c.c.} \tag{4.20}$$

This solution shows that $\psi_1^{(s)}$ has a phase advance of $\pi/2$ with respect to the wall profile, and hence the flow in the vicinity of the boundary is directed from trough to crest ($\partial_z^2(\chi + \chi^*)|_{z=0} > 0$). By shifting the coordinate system along the x-axis we can change the phase of the wall profile so as to make it a simple cosine function. We consider $\eta(x) = \cos(kx)$ in what follows.

Following Lyne (1971), we now proceed to study the limits of k large and small, while $kRe \ll 1$. For $k \gg 1$ the wavelength of the boundary profile is much smaller than the thickness of the viscous layer. In this case, a boundary layer appears of characteristic thickness $1/k$. Screening between regions producing positive and negative vorticity

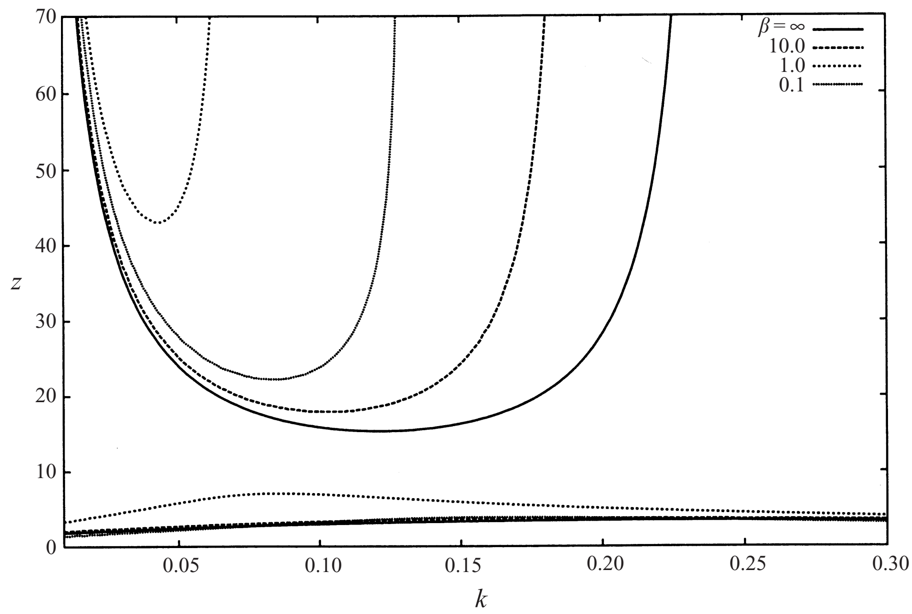

FIGURE 6. The lines indicate the values of z at which $u_1^{(s)} = 0$ as a function of the boundary wavenumber k, and for a range of values of β. At fixed k, the flow can have one ($k > 0.23$) or two ($0 < k \leqslant 0.23$) recirculating cells ahead of the boundary. Note that the location of the second recirculating cell strongly depends on β.

occurs over a distance much smaller than the Stokes thickness based on the frequency of oscillation. The net vorticity does not diffuse even to distances of $z \sim O(1)$, hence giving rise to exponential decay with an $\exp(-kz)$ factor. The region in which the stream function is not exponentially small depends on $Z = kz$. The explicit form of $\psi_1^{(s)}$ may be obtained by direct expansion of the solution (4.20) in power series of $1/k$, keeping Z fixed. The leading contribution to the steady part of the tangential component of the velocity is given by

$$u_1^{(s)} = k\partial_Z \psi_1^{(s)} \sim -\frac{Re}{24k^2} \sin(kx)\, e^{-Z} Z(6 - Z^2). \tag{4.21}$$

The boundary layer comprises two recirculating cells per wall period, located within $0 < z \lesssim 1/k$. $u_1^{(s)}$ changes sign at $z = 6^{1/2}/k$.

In the opposite limit of $k \ll 1$ one formally recovers the Schlichting problem in that the characteristic longitudinal length scale is much larger than the Stokes layer thickness. There is one fundamental difference, however, which can be seen from the solution, (4.18). It has two contributions. The first one is proportional A_i, arises from the particular solution, and serves to balance the non-homogeneity in (4.16). This contribution decays within the Stokes layer. The second one is proportional to B_i, and arises from the general solution of the homogeneous part of the equation. This contribution decays over the stretched scale Z. It turns out that this second contribution introduces an additional change of sign in the velocity when $0 < k \leqslant 0.23$, hence allowing two or four recirculating cells per period ahead of the boundary. The location of $u_1^{(s)} = 0$ as a function of k is shown figure 6. The location of the second recirculating cell is entirely determined by that part of the solution that is proportional to B_i, and occurs at $z \sim O(1/k) \gg 1$.

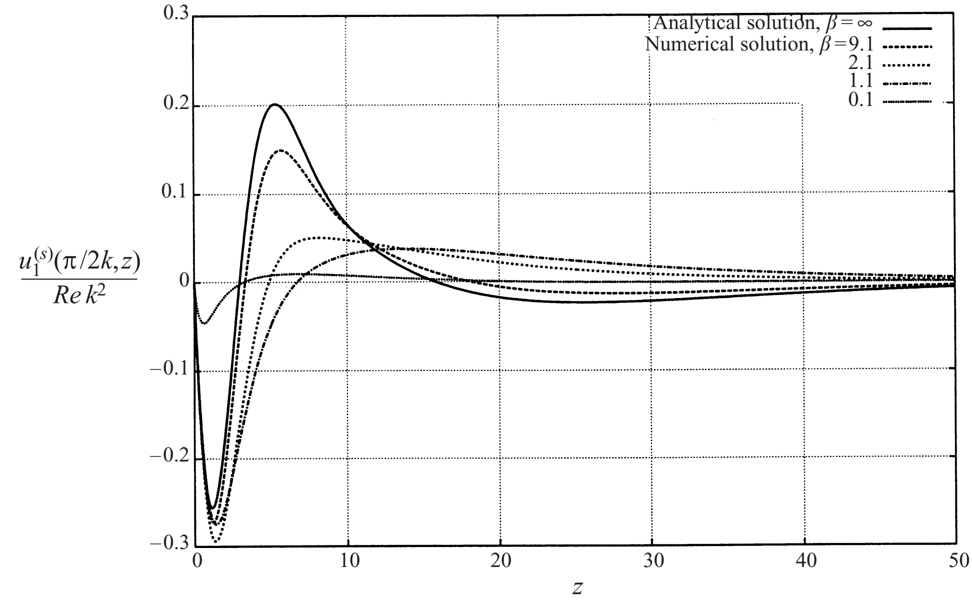

FIGURE 7. Tangential component of the mean stationary velocity as a function of z for $k = 0.1$ and a range of values of β. The case $\beta = \infty$ corresponds to the analytic solution obtained by Lyne. The other curves are the numerical solutions of the boundary value problem defined by (4.16) and corresponding boundary conditions.

The steady velocity may be obtained by expanding the exact solution (4.18) in power series of k, first keeping z fixed (inner solution, $u_{1i}^{(s)}$), and second keeping Z fixed (outer solution $u_{1o}^{(s)}$). To leading order, we find,

$$u_{1i}^{(s)}(z') \sim -Rek^2 \sin(kx)\{[\tfrac{1}{2}z'(\sin(z') - \cos(z')) + 2\sin(z') + \tfrac{1}{2}\cos(z')]e^{-z'} + \tfrac{1}{4}e^{-2z'} - \tfrac{3}{4}\}, \quad z' = z/2^{1/2} \sim O(1), \tag{4.22}$$

$$u_{1o}^{(s)}(Z) \sim -Rek^2 \sin(kx)[\tfrac{3}{4}(Z-1)e^{-Z}], \qquad Z \sim O(1). \tag{4.23}$$

The solution for the inner and outer steady velocities has already been obtained by Lyne (1971) by a conformal transformation technique. We further note that the inner and outer solutions can now be matched by requiring that $u_{1i}^{(s)}(\infty) = u_{1o}^{(s)}(0) = (3/4)Rek^2\sin(kx)$. Hence it is possible to construct a uniformly valid solution by adding the inner and outer solutions, and subtracting the first term of the inner expansion of the outer solution. Our final result, valid in the deterministic limit, is

$$u_{1c}^{(s)}(z') \sim -Rek^2 \sin(kx)\{[\tfrac{1}{2}z'(\sin(z') - \cos(z')) + 2\sin(z') + \tfrac{1}{2}\cos(z')]e^{-z'} + \tfrac{1}{4}e^{-2z'} + \tfrac{3}{4}(2^{1/2}kz' - 1)\exp(-2^{1/2}kz')\}. \tag{4.24}$$

We next turn to a numerical study of the case of finite β. The boundary value problem (4.16) has been solved numerically by using a multiple shooting method for non-stiff and linear boundary value problems (Mattheij & Staarink 1984). The method has the advantage that the necessary intermediate shooting points are determined by the method itself, and that it can give the solution on a preset and non-uniform grid of points. The code was tested on the analytically known solution of the deterministic limit, (4.18) and (4.19). Our results are summarized in figures 6, 7 and 8.

Figure 6, already discussed above, shows that for fixed k, the mean stationary

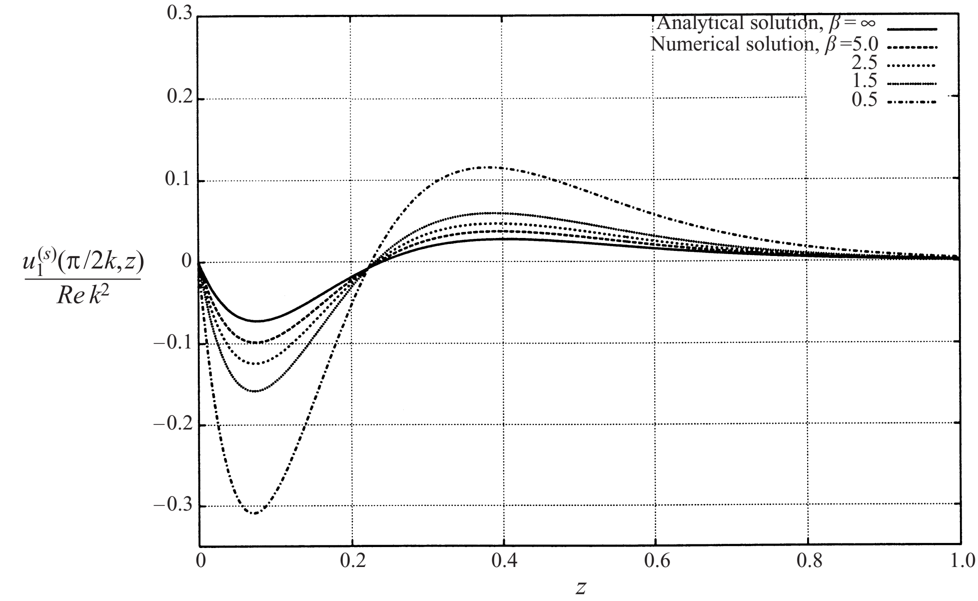

FIGURE 8. Tangential component of mean stationary velocity as a function of z for $k = 10$ and a range of values of β. The case $\beta = \infty$ corresponds to the analytic solution obtained by Lyne. The other curves are the numerical solutions of the boundary value problem defined by (4.16) and corresponding boundary conditions.

velocity field may be composed of two or four recirculating cells per wall period depending on β. The location of the first is largely independent of β, whereas the deviation of the second relative to its location in the monochromatic limit is proportional to $\beta/\pi(1+\beta^2)$, the value of $P(0,\beta)$.

Our results in the limit $k \ll 1$ are presented in figure 7, where profiles of tangential component of the mean stationary velocity are plotted for $k = 0.1$ and different values of β. At large β (close to the monochromatic limit) the flow is composed of four recirculating cells per boundary period. Upon decreasing β, the location of the second pair of recirculating cells moves to infinity (see also figure 6), so that beyond some critical value of β, only two recirculating cells remain. Further decrease in β results in the reappearance of a pair of recirculating cells at infinity, which then continue to move towards decreasing z. The intensity of the recirculating modes does not change monotonically with β as we further discuss below. We also note that for sufficiently small k (a factor of ten or more smaller than the value of $k = 0.1$ shown in figure 7), $u_1^{(s)}$ decays very slowly between $z \sim O(1)$ and $z \sim O(1/k)$. This rate of decay has the same physical origin as the logarithmic divergence discussed in § 3. The velocity $u_1^{(s)}$ finally crosses over to exponential decay for $z > O(1/k)$.

In the opposite limit of $k \gg 1$ (figure 8 shows the case $k = 10.0$; note that $u_1^{(s)}$ is now normalized by Re/k^2), the qualitative structure of the flow is largely independent of β. The streaming flow has two recirculating cells per wall wavelength, and their intensity increases monotonically with decreasing β.

The complex dependence of the flow on β and k can be qualitatively understood from the interplay between the width of the power spectrum (given by $1/\beta$), the viscous damping of each elementary excitation that depends on its frequency, and the penetration depth of the flow field which is primarily dictated by the boundary wavelength. For small k, large-frequency modes are damped close to the boundary and do not penetrate much into the recirculating layers. Reducing β introduces high-frequency components into the driving terms at first order, but they are dynamically damped. At the same time, the power in the dominant frequency components (around Ω) decreases. Overall, a decrease in β then leads to a decrease in recirculation strength. As k increases, larger frequencies contribute to the flow over the entire range of the recirculating cells. Decreasing β decreases the strength of the dominant components, but increases the range of high frequencies that can contribute to the flow. From (4.16) one can show that the driving contribution from higher frequencies which is contained in Q increases faster with frequency than the decreasing weight given to them by the power spectrum $P(\omega, \beta)$. Consequently, decreasing β (which amounts to moving towards the white noise limit) leads to increasing amplitude of the recirculation.

In summary, for any value of β, finite or infinite, the vorticity produced by vibration of the wavy boundary does not penetrate into the bulk farther than a distance of order of the wavelength of the boundary. However, there are qualitative differences with the deterministic limit in the character of the flow within that layer. In particular, the structure and the intensity of the stationary secondary flow strongly depend on β.

5. Summary

We have addressed the flow induced by a randomly vibrating solid boundary in an otherwise quiescent fluid. This analysis has been motivated by the random residual acceleration field in which microgravity experiments are conducted. The salient features of the flow are summarized below.

When the solid boundary is planar, the flow field averages to zero (the average velocity of the boundary has been taken to be zero in all cases investigated), but its variance decays algebraically with distance away from the wall. This dependence follows from a non-vanishing power spectrum of the boundary velocity at zero frequency. Introducing a low-frequency cut-off in the power spectrum leads back to the classical exponential decay, with a rate that is determined by the cut-off frequency, (2.19). The amplitude of the decaying variance depends explicitly on the correlation time of the boundary velocity, $\beta = \Omega\tau$, where Ω is the dominant angular frequency of the power spectrum of the boundary velocity, and τ is inverse spectral width (τ is the correlation time of the boundary velocity).

If the solid boundary is weakly curved, steady streaming is generated in analogy with the classical analysis of Schlichting. The stationary part of the ensemble average of the secondary velocity is non-zero, even though the boundary velocity averages to zero. In this case, we find that the leading contribution to the average stationary velocity diverges logarithmically with distance away from the boundary. In analogy to the planar case, the introduction of a low-frequency cut-off in the power spectrum of the boundary velocity changes the asymptotic behaviour qualitatively. The average stationary velocity asymptotes now to a constant, given by (3.18). The asymptotic velocity explicitly depends on β and logarithmically on the cut-off frequency. This asymptotic behaviour is not reached until a length scale of the order of the Stokes layer thickness that is based on the cut-off frequency.

We have finally analysed the case of a periodically modulated solid boundary in the limit in which the scale of the wall modulation is small compared to the thickness of the Stokes layer, and also when the spatial amplitude of the boundary oscillation is small compared with the wavelength of the wall profile. Cancellation of vorticity production over the wall boundary leads to exponential decay of the fluid velocity away from the boundary, with a decay length which is proportional to the wall wavelength, even if the zero frequency value of the power spectrum of the boundary velocity is non-zero. If the boundary wavelength is much larger than the Stokes layer thickness, we find steady streaming in secondary flow with two or four recirculating cells per wall period depending on β. On the other hand, if the wavelength is much smaller than the Stokes layer thickness, only two recirculating cells are formed regardless of the value of β. Somewhat unexpectedly, the intensity of the recirculation can both increase or decrease with β.

This research has been supported by the Microgravity Science and Applications Division of the NASA under contract No. NAG3-1885, and also in part by the Supercomputer Computations Research Institute, which is partially funded by the US Department of Energy, contract No. DE-FC05-85ER25000.

Appendix. Transient layer formation

In the two limiting cases of white and monochromatic noise, it is possible to find an analytic solution for the transient flow induced by a vibrating planar boundary in an otherwise quiescent fluid. The retarded, infinite-space Green's function for equation (2.1), with boundary conditions (2.2), is

$$G(z,t|z',t') = \frac{1}{(4\pi\nu(t-t'))^{1/2}}[\exp[-(z-z')^2/4\nu(t-t')] - \exp[-(z+z')^2/4\nu(t-t')]], \quad t > t', \qquad \text{(A 1)}$$

and $G(z,t|z',t') = 0$ for $t < t'$. If the fluid is initially quiescent, $u(z,0) = 0$, we find

$$u(z,t) = \nu \int_0^t \mathrm{d}t'\, u_0(t')\, (\partial_{z'} G)_{z'=0}\,. \qquad \text{(A 2)}$$

If $u_0(t)$ is a Gaussian, white noise process, the ensemble average of (A 2) yields $\langle u(z,t)\rangle = 0$. The corresponding equation for the variance reads

$$\left\langle u^2(z,t)\right\rangle = 2D\nu^2 \int_0^t \mathrm{d}t'\ [(\partial_{z'} G)_{z'=0}]^2 = \frac{2D\nu}{\pi z^2}\left(1 + \frac{z^2}{2\nu t}\right)\exp\left(-z^2/2\nu t\right). \qquad \text{(A 3)}$$

The variance of the induced fluid velocity propagates into the fluid diffusively. Saturation occurs for $t \gg z^2/2\nu$, at which point the variance does not decay exponentially far away from the wall, but rather as a power law $\left\langle u^2(z,\infty)\right\rangle = 2D\nu/\pi z^2$. The divergence as $z \to 0$ is a spurious consequence of the white noise limit considered. See (2.15) for the limiting behaviour at finite correlation time of the noise.

Consider now the opposite limit of monochromatic noise with correlation function

$$\langle u_0(t)u_0(t')\rangle = \left\langle u_0^2\right\rangle \cos\left[\Omega(t-t')\right]. \qquad \text{(A 4)}$$

Now using (A 2) and (A 4) we find (Carslaw & Jaeger 1959)

$$\frac{\left\langle u^2(z,t)\right\rangle}{2\left\langle u_0^2\right\rangle} = \frac{2}{\pi}\int_\kappa^\infty \mathrm{d}\sigma\, \mathrm{e}^{-\sigma^2} \int_\kappa^\infty \mathrm{d}\mu\, \mathrm{e}^{-\mu^2} \cos\left[\frac{z^2}{2\delta_s^2}\left(\frac{1}{\mu^2} - \frac{1}{\sigma^2}\right)\right], \qquad \text{(A 5)}$$

with $\kappa = z/(4\nu t)^{1/2}$. A closed form solution can only be obtained for long times. We find

$$\frac{\left\langle u^2(z,t)\right\rangle}{2\left\langle u_0^2\right\rangle} = \frac{\exp\left(-2z/\delta_s\right)}{2} + \frac{2\kappa^3\delta_s^2}{\pi^{1/2}z^2}\exp\left(-z/\delta_s\right)\sin(\Omega\, t - z/\delta_s) + O(\kappa^5(t)). \qquad \text{(A 6)}$$

At long times, the variance propagates into the bulk with phase velocity $(2\nu\Omega)^{1/2}$, while its amplitude decays exponentially in space over the scale of the Stokes layer, and as $t^{-3/2}$ in time. In summary, the flow created by the vibration of the boundary propagates diffusively for white noise ($z^2 \propto 2\nu t$), and as a power law ($z^2 \propto \pi\nu\Omega^2 t^3$) in the monochromatic limit.

REFERENCES

ALEXANDER, J. I. D. 1990 Low-gravity experiment sensitivity to residual acceleration: a review. *Microgravity Sci. Technol.* **3**, 52.

ALEXANDER, J. I. D., GARANDET, J. P., FAVIER, J. J. & LIZEE, A. 1997 g-jitter effects on segregation during directional solidification of tin-bismuth in the mephisto furnace facility. *J. Cryst. Growth* **178**, 657.

ALEXANDER, J. I. D., OUAZZANI, J. & ROSENBERGER, F. 1991 Analysis of the low gravity tolerance of Bridgman-Stockbarger crystal growth. *J. Cryst. Growth* **113**, 21.

BATCHELOR, G. K. 1967 *An Introduction to Fluid Dynamics*. Cambridge University Press.

BLONDEAUX, P. & VITTORI, G. 1994 Wall imperfections as a triggering mechanism for Stokes layer transition. *J. Fluid Mech.* **264**, 107.

CARSLAW, H. S. & JAEGER, J. C. 1959 *Conduction of Heat in Solids*. Clarendon Press.

DELOMBARD, R., MCPHERSON, K., MOSKOWITZ, M. & HROVAT, K. 1997 Comparison tools for assessing the microgravity environment of missions, carriers and conditions. *Tech. Rep.* TM 107446. NASA.

FAROOQ, A. & HOMSY, G. M. 1994 Streaming flows due to g-jitter-induced natural convection. *J. Fluid Mech.* **271**, 351.

GERSHUNI, G. Z. & LYUBIMOV, D. V. 1988 *Thermal Vibrational Convection*. John Wiley & Sons.

GERSHUNI, G. Z. & ZHUKHOVITSKII, E. M. 1976 *Convective Stability of Incompressible Fluids*. Jerusalem: Keter.

GRADSHTEYN, I. S. & RYZHIK, I. M. 1980 *Tables of Integrals, Series and Products*. Academic Press.

GRASSIA, P. & HOMSY, G. M. 1998*a* Thermocapillary and buoyant flows with low frequency jitter. I. jitter confined to the plane. *Phys. Fluids* **10**, 1273.

GRASSIA, P. & HOMSY, G. M. 1998*b* Thermocapillary and buoyant flows with low frequency jitter. II. spanwise jitter. *Phys. Fluids* **10**, 1291.

KAMOTANI, Y., PRASAD, A. & OSTRACH, S. 1981 Thermal convection in an enclosure due to vibrations aboard a spacecraft. *AIAA J.* **19**, 511.

KANEKO, A. & HONJII, H. 1979 Double structures of steady streaming in the oscillatory viscous flow over a wavy wall. *J. Fluid Mech.* **93**, 727.

LYNE, W. H. 1971 Unsteady viscous flow over a wavy wall. *J. Fluid Mech.* **50**, 33.

MATTHEIJ, R. M. M. & STAARINK, G. W. M. 1984 An efficient algorithm for solving general linear two-point bvp. *SIAM J. Sci. Statist. Comput.* **5**, 745.

NAYFEH, A. H. 1981 *Introduction to Perturbation Techniques*. John Wiley & Sons.

NELSON, E. S. 1991 An examination of anticipated g-jitter on space station and its effects on materials processes. *Tech. Rep.* TM 103775. NASA.

SCHLICHTING, H. 1932 Berechnung ebner periodischer Grenzschichtströmungen. *Phys. Z.* **33**, 327.

SCHLICHTING, H. 1979 *Boundary Layer Theory*, 7th edn. McGraw-Hill.

STOKES, G. G. 1851 On the effect of the internal friction of fluids on the motion of pendulums. *Camb. Trans.* **ix**[8] (*Papers*, **iii**.1).

STRATONOVICH, R. L. 1967 *Topics in the Theory of Random Noise*, vol. II. Gordon and Breach.

THOMSON, J. R., CASADEMUNT, J., DROLET, F. & VIÑALS, J. 1997 Coarsening of solid-liquid mixtures in a random acceleration field. *Phys. Fluids* **9**, 1336.

VAN DYKE, M. 1964 *Perturbation Methods in Fluid Mechanics*. Academic Press.

VITTORI, G. 1989 Non-linear viscous oscillatory flow over a small amplitude wavy wall *J. Hydr. Res.* **27**, 267.

WALTER, H. U. (ED.) 1987 *Fluid Sciences and Materials Sciences in Space*. Springer Verlag.

ZHANG, W., CASADEMUNT, J. & VIÑALS, J. 1993 Study of the parametric oscillator driven by narrow band noise to model the response of a fluid surface to time-dependent accelerations. *Phys. Fluids* A **5**, 3147.